Chemical Engineering Journal 94 (2003) 189–198

Chemical Engineering Journal

www.elsevier.com/locate/cej

Analysis of axial dispersion in an oscillatory-flow continuous reactor

Mauri Palma, Reinaldo Giudici*

Departamento de Engenharia Química, Universidade de São Paulo, Escola Politécnica, Caixa Postal 61548, CEP 05424-970 Sao Paulo, SP, Brazil

Received 26 July 2002; accepted 8 February 2003

Abstract

Experimental results of axial mixing for single-phase flow in pulsed sieve plate column (PSPC) were presented and discussed. The study is aimed at the use of the PSPC as a new type of oscillatory-flow tubular reactor for emulsion polymerization processes. The effects of pulsation frequency and amplitude, flow rate, plate spacing and fluid viscosity were studied. Axial dispersion coefficients were determined by fitting the axial dispersion model to the measurements of residence time distribution. A total of 213 runs were carried out with water at 20 °C, covering the range of pulsation frequency from 0 to 4.5 s^{-1}, amplitude of pulsation from 5 to 25 mm, plate spacing 25, 50 and 100 mm, and water flow rate from 3.8 to 11.8 l/h. The results show that, under absence of pulsation, axial dispersion increases with flow rate and exhibits a maximum with respect to the plate spacing. For pulsed (oscillatory) flow, axial dispersion coefficient increases with amplitude and frequency of pulsation, and the effect of plate spacing is dependent of the pulsation velocity. Additional 39 experiments for pulsed flow were performed with aqueous solution of poly(vinyl alcohol) with viscosity varying in the range 1.4–10.0 cP. The results show that the axial dispersion decreases with plate spacing, increases with the viscosity for plate spacing 25 mm and is nearly independent of viscosity for plate spacing 50 and 100 mm. A correlation proposed in the literature was tested.

Keywords: Axial dispersion; Oscillatory-flow reactor; Single-phase flow

1. Introduction

Industrial emulsion polymerization is mostly carried out in stirred tank reactors operated in batch or semibatch modes. To meet future requirements of tighter product specifications, lower environmental pollution, reduced production costs, and to reduce batch-to-batch variations, the use of small continuous reactors may be a potential alternative to replace semibatch processes. Reactors with broad residence time distributions, such as continuous stirred tanks and loop tubular reactors, show sustained oscillations in particle number and conversion as was shown by Greene et al. [1] and Kiparissides et al. [2]. Pulsed tubular reactors can avoid this oscillatory behavior, and present interesting features, such as intense radial mixing and good heat transfer (high area-to-volume ratio) as shown by Hoedemakers [3] and Paquet and Ray [4].

In the present work, a new type of oscillatory-flow tubular reactor, the pulsed sieve plate column (PSPC) has been studied with respect to the axial mixing. The perforated plates coupled with the pulsed (oscillatory) flow may promote excellent radial mixing and controllable axial dispersion. Good radial mixing favors the heat removal, which plays an important role in polymerization reactors. The control of axial dispersion allows one to operate the PSPC in wide range of backmixing behavior, from an almost continuous stirred tank reactor (CSTR) to an almost plug flow reactor (PFR). The control of axial dispersion in continuous emulsion polymerization reactor is very interesting because particle size distribution (PSD), one of the most important characteristics of an emulsion, is strongly influenced by the axial dispersion (PSD is narrow in an ideal PFR and broad in a CSTR).

The performance of a PSPC has been experimentally investigated with the objective to characterize the axial dispersion for a single-phase flow in this system, as a function of pulsation frequency, stroke length of pulsation, flow rate, and distance between plates. Dispersion coefficients were obtained from residence time distribution (RTD) measurements in the equipment. RTD is an important tool for the analysis of real reactors, to detect and quantify non-ideal flow patterns in chemical reactors. Deviations from the ideal plug flow behavior can arises different causes, such as, the presence of stagnant regions (dead zones), and the presence of regions which offer little resistance to flow (channeling, by-passing, or short circuit). Additional secondary mechanisms that may cause mixing, as pointed out by

* Corresponding author. Tel.: +55-11-3091-2254; fax: +55-11-3813-2380.
E-mail address: rgiudici@usp.br (R. Giudici).

1385-8947/03/$ – see front matter © 2003 Elsevier B.V. All rights reserved.
doi:10.1016/S1385-8947(03)00057-3

Nomenclature

a	parameter in Eq. (7)
A	pulsation amplitude (m)
b	parameter in Eq. (7)
c	tracer concentration (kg/m^3)
c_F	tracer concentration in fluid flux (kg/m^3)
c_{IFF}	tracer concentration for a Dirac delta injection type (kg/m^3)
C_D	drag coefficient in the holes (Eq. (8))
d_0	hole diameter (m)
d_{PS}	spherical particle diameter (m)
D	column diameter (m)
D_{ea}	axial dispersion coefficient (m^2/s)
D^0_{ea}	axial dispersion coefficient for zero flow rate (m^2/s)
e	fractions of free area in the plates
f	pulsation frequency (s^{-1})
F	function
g	gravitational constant (m/s^2)
h	plate spacing (m)
l	Prandtl mixing length (m)
L	column length (m)
M	total amount of tracer injected (kg)
P	power dissipation (W/kg)
Pe	Peclet number for a column of length L ($Pe = uL/D_{ea}$)
Q	flow rate (l/h)
R	net reaction rate (kg/m^3 s)
S	cross-sectional area of the column (m^2)
t	time (s)
u	superficial velocity (m/s)
u_S	settling velocity (m/s)
V	column section volume (m^3)
z	axial position (m)

Greek letters

$\delta(t)$	Dirac delta function for time variable (s^{-1})
μ_C	viscosity of the continuous phase (kg/m s)
ρ_C	density of the continuous phase (kg/m^3)
ρ_M	monomer density (kg/m^3)
ρ_P	polymer density (kg/m^3)
ρ_{PS}	density of spherical particle (kg/m^3)
$\sigma_{D_{ea}}$	S.D. of axial dispersion coefficient (m^2/s)
σ_f	S.D. of pulsation frequency (s^{-1})
σ_Q	S.D. of flow rate (l/h)

Subscripts

C	continuous phase
m	mean value
M	monomer
P	polymer
PS	spherical particle
S	settling

Pratt and Baird [5] and Qader et al. [6], are: molecular and turbulent diffusion in both radial and axial directions; non-flat velocity profile; dispersion of particles due to differences in terminal velocities; flow maldistribution inside the reactor.

RTD curves are usually obtained from stimulus-response experiments, in which the concentration of a substance (named tracer) at the inflow is disturbed, and the response at the reactor exit is measured. The tracer is usually an inert compound, which behaves like the fluid flowing in the reactor.

From the RTD analysis, it is possible to obtain parameters that characterize the flow dispersion by fitting parameters of a model representing the flow in the reactor. These parameters are usually dependent on the fluid properties, the vessel geometry, and the flow nature.

2. Axial dispersion model

The axial dispersion model, also called axially dispersed plug flow model, is usually employed to describe non-ideal tubular flow. It is assumed that, superimposed to the main flow, there exists an axial mixing of material which is governed by an analogous to the Fick's law of diffusion. The axial mixing is characterized by the axial dispersion coefficient, D_{ea}, mathematically analogous to, but physically different, from the molecular diffusion coefficient. The axial coefficient can be expressed by the dimensionless Peclet number ($Pe = uL/D_{ea}$), where u is the average superficial flow velocity and L is the column length. Mecklenburgh and Hartland [7] presented a rigorous theoretical treatment on axial mixing.

The axial dispersion model is mathematically described by Levenspiel and Bischoff [8]

$$\frac{\partial c}{\partial t} = -u\frac{\partial c}{\partial z} + D_{ea}\frac{\partial^2 c}{\partial z^2} + R \tag{1}$$

where c is the concentration, t the time, z the axial position, and R the net reaction rate. The second term in the right-hand side of Eq. (2) represents the axial dispersion, in a form mathematically analogous to the Fick's law of diffusion, that is, the flux is proportional to the concentration gradient. The dispersion coefficient D_{ea}, is an effective parameter that accounts for the effect of different causes of axial mixing (e.g. non-uniform velocity profile, molecular diffusivity, turbulence, presence and type of internals that causes a flow pattern, etc.).

In order to determine D_{ea}, data obtained from transient stimulus-response experiments can be used in a fitting model procedure. For the case considered in the present study, with no reaction occurring during the RTD runs, the corresponding reaction term (R) was excluded from Eq. (1). The adequate boundary conditions are that for semi-infinite column with injection and detection in flux, proportional to the flow

as pointed out by Kreft and Zuber [9]:

$$c_F(0,t) = \frac{M}{Sz}\delta(t) \quad (2)$$

$$c_F(z,0) = 0 \quad (3)$$

$$\lim_{z\to\infty} c_F(z,t) = 0 \quad (4)$$

Considering the work of Kreft and Zuber [9] one can conclude that the boundary conditions given by Eqs. (2)–(4) apply to our case, that is, for infinite media or "open–open" boundary conditions, because "if there is no transport by molecular diffusion through the injection cross-section, the existence or non-existence of the dispersive medium from 0 to $-\infty$ has no influence on the discussed solutions". In the equipment used, the feeding pipe is located at about 75 mm above the center of the pulsator travel length (50 mm from uppermost position of the pulsator surface), and close to (less than 10 mm from lower position) the first sieve plate. The flow at this feeding position (slightly below the first plate) is expected to have similar hydrodynamic behavior as that in the remainder of the column. This justifies the choice of open-boundary condition at the bottom of the column. The "zigzag" in the lateral surface of the expansion joint favors some turbulence at the region below the first plate.

In Eqs. (2)–(4) c_F is the tracer concentration in feed flow, M the total amount of tracer injected, $\delta(t)$ the Dirac delta function (a peak at time $t = 0$) and S the cross-sectional area of the column. Theoretically, the pulse-like injection of tracer is mathematically described by a Dirac's delta function. In the experiments, the injection of tracer was made in very short times (1–2 s) if compared to the mean residence time (5–15 min), so that the tracer injection can be for all purposes considered instantaneous.

The solution of Eq. (1) for the tracer concentration at the column exit after a perfect pulse (Dirac's delta) tracer input at time $t = 0$, is given by Kreft and Zuber [9] as:

$$c_{IFF} = \frac{M}{V}\frac{1}{((4\pi D_{ea}/L^4)u^2t^3)^{1/2}}\exp\left(\frac{-(1-ut/L)^2}{4D_{ea}t/L^2}\right) \quad (5)$$

where c_{IFF} is the tracer concentration at the reactor exit, V the column section volume and L the column section length between the injection point ($z = 0$) and the detection point ($z = L$).

The approach for determining the effective dispersion coefficient D_{ea} was to fit the model, Eq. (5), to the experimental measurements of the residence time distribution. In Eq. (5), M/V and u, may also be treated as model parameters. Preliminary tests performed by the authors have shown that this procedure, with three adjustable parameters, give values of axial dispersion coefficient more reliable than the usual models where D_{ea}, (or Pe) is the only fitted parameter.

In a previous work, Brunello et al. [10] have determined the axial dispersion coefficients for the same equipment and conditions used here, but only for water and plate spacing of 25 and 50 mm. Brunello et al. [10] used the axial dispersion model, but with the "closed–closed" boundary conditions discussed by Wen and Fan [11]. However, it must be pointed out that the estimates of Pe using Eq. (5) does not differ significantly from estimates using "closed–closed" boundary conditions as given by Gouvea et al. [12]. Preliminary results of the present study were first presented by Palma and Giudici [13].

3. Previous works on axial dispersion in PSPC

PSPCs were patented by Van Dijk [14] and have been most used for liquid–liquid extraction in different applications of two-phase flow as shown by Logsdail and Slater [15].

In the present work, a PSPC is studied for application as a continuous reactor for emulsion polymerization. In this system, the monomer droplets typically size from 10^{-6} to 10^{-5} m, the polymer particle size are typically in the range 10^{-8} to 10^{-7} m and micelle are typically in the range 1×10^{-9} to 5×10^{-9} m, therefore they are very small and are stabilized by emulsifier as shown by Hoedemakers [3]. Due to the agitation provided by the pulsation and the sieve-plates, there is enough radial mixing to prevent the droplets coalescence. An estimate of Stokes settling velocity of micelles, polymer particles, and monomer droplets, can be done using Eq. (6), as in Paquet and Ray [4]:

$$u_S = \frac{d_{PS}^2(\rho_{PS} - \rho_C)g}{18\mu_C} \quad (6)$$

Applying Eq. (6) for a typical emulsion polymerization of vinyl acetate at 55 °C (densities of monomer, polymer and water are respectively $\rho_M = 0.93\,g/cm^3$, $\rho_P = 1.15\,g/cm^3$, $\rho_C = 1.0\,g/cm^3$, and water viscosity is $\mu_C = 0.56\,cP$) results in settling velocities lower than 6.5×10^{-7} cm/s. For typical mean residence times of 1 h, buoyancy effects are clearly negligible for polymer particles and micelles. Under these conditions, the fluid flowing through the column can be considered single phase.

Only few authors have studied axial dispersion for single-phase flow in PSPCs, namely Miyauchi and Oya [16], Novotny et al. [17], Baird [18], Rao et al. [19], Godfrey et al. [20] and Ingham et al. [21]. These studies provide a good starting point for better understanding of the more complex two-phase systems as well as for the development of better correlations. Literature data on single-phase axial dispersion in PSPC have been correlated as a function of column diameter (D), geometric characteristics of the plate, such as hole diameter (d_0), fractional plate free area (e) and plate spacing (h); operating conditions, such as pulsation frequency (f), pulsation amplitude (A), and superficial flow velocity (u); and fluid properties, density (ρ_C), and viscosity (μ_C).

Ingham et al. [21] obtained the following empirical equation for the axial dispersion coefficient in PSPCs at zero flow rate:

$$D^0_{ea} = a\left(\frac{\rho_C d_0 fA}{\mu_C}\right)^{-0.3}(fA)(1-e^2)\frac{D^{1.33}}{(he^2C_D^2)^{0.33}} + b\left(\frac{fA^2}{e^2}\right)\left(\frac{h}{A}\right)^{0.45} \quad (7)$$

where D^0_{ea} is the axial dispersion coefficient at zero flow rate, that is, only caused by pulsation, a and b are empirical constants for the effects of axial mixing close to the plates and those in the main body of the column compartments, whose values are given for different geometry, C_D is the drag coefficient in the holes, which is a function of the Reynolds number based on plate hole size:

$$C_D = F\left(\frac{\rho_C d_0 fA}{\mu_C}\right) \quad (8)$$

However, those authors suggested the use of $C_D = 0.6$ instead of Eq. (8).

The influence of the continuous phase velocity is given, based on a theoretical basis, by the equation proposed by Miyauchi and Oya [16]:

$$D_{ea} = D^0_{ea}\left(1 + \frac{u}{2fA}\right) \quad (9)$$

Ingham et al. [21] worked with PSPCs with the following features: column diameters, 40, 76, 101 and 152 mm; effective length 0.8, 1, 1.5, 2 and 3 m; plate free area 17 and 22%; plate hole diameter 3 and 3.2 mm; plate spacing 23–192 mm. The pulsation covered the range of amplitudes from 4 to 240 mm and frequencies from 0.3 to 3.2 s^{-1}. Their results showed that, for the same fluid, geometric characteristics and operating conditions, the axial dispersion is most affected by the pulsation amplitude and frequency, and plate spacing. This strong influence of plate spacing was also observed by Nabli et al. [22] for a disk-and-doughnuts column similar to a PSPC.

The experimental values of axial dispersion coefficient obtained by Ingham et al. [21] are in the range 10^{-4} to 10^{-3} m^2/s. These values are similar to those obtained by Meuldijk et al. [23], 0.84×10^{-4} to 3×10^{-4} m^2/s, in a pulsed column packed with Raschig rings. According to Meuldijk et al. [23], the control of axial dispersion under this range, during the vinyl acetate emulsion polymerization in a pulsed packed column, allows stable operation of the reactor, eliminating the oscillations in monomer conversion and number of particles, those typically are observed in well-mixed continuous reactors.

4. Experimental setup and procedure

The equipment used in the present work is presented schematically in Fig. 1 and is similar to those used by Palma [24], Meuldijk et al. [23], Mayer et al. [25,26] and Brunello et al. [10].

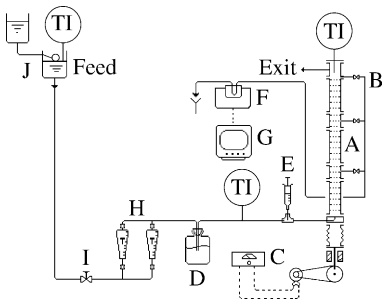

Fig. 1. Schematic of experimental setup. A: PSPC; B: sampling probe; C: pulsator; D: pulse damper; E: tracer injection; F: spectrophotometer; G: computer and data acquisition system; H: rotameters; I: valve; J: feeding tanks.

The column A is made of three glass tube sections of length 800 mm and internal diameter 39.6 mm. A sampling probe is installed at the end of each glass section and consist of a 3 mm tube perpendicularly connected to the column wall. Axial positions of the sampling line connections are 870, 1748 and 2616 mm downstream from the feed point. Sampling line is a 3 mm diameter tube and about 3 m long from the sampling point to the spectrophotometer cuvette. The plates are made of stainless steel, with 39 holes of 3 mm diameter in triangular arrange, resulting in a free area of 22.3%. Pulsation is provided by a pulsator, C, made by a teflon expansion linked to an excentric rotor and a continuous current electric motor. A variac allows one to adjust the pulsing frequency from 0.2 to 4.5 s^{-1}, the pulsing amplitude can be varied from 5 to 25 mm. The flow rate ranged from 4 to 12 l/h of water. Plate spacing was changed to 25, 50 and 100 mm. Temperature was kept in $20 \pm 1\,^{\circ}C$ in all experiments here reported. Water in the feeding tanks was kept at 20 °C and temperature was continually monitored at the column inlet and at the column outlet streams. Runs in which any measured temperature was out of the range $20 \pm 1\,^{\circ}C$ were discarded.

Water flows from the tanks, J, with flow rates were regulated by valve, I, and measured by a rotameter, H. Close to the column feeding, a tee, E, allows the injection of the tracer, a 0.3% methylene blue solution. The injected volume was 0.05 ml. This amount was determined from previous experiments in order to provide tracer concentrations at the spectrophotometer in the recommended accurate range.

Residence time distribution is measured on-line by continuously sampling through the sampling line, B, followed by a spectrophotometer, F, connected to a computer for automatic data acquisition. In all cases, sampling flow rate (1.6–3.5 l/h) was regulated to a value lower than half of the total flow rate in the column (4–12 l/h). Time data for each run was shifted by the mean residence time in the sampling line (50–120 s). Dispersion in the sampling line (diameter 3 mm and volume 21 cm^3) was measured also by

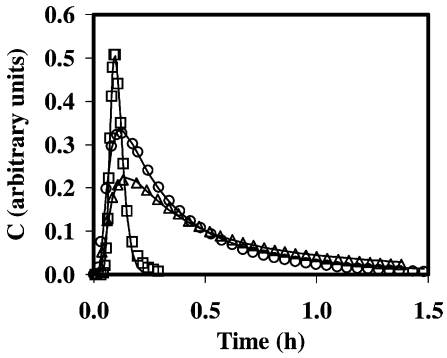

Fig. 2. Measured and calculated response curves. The lines correspond to curves calculated with Eq. (5), with fitted D_{ea} values. Numerical values of concentration was adopted equal to the absorbance values directly indicated by the spectrophotometer.

stimulus-response methodology and result was negligible in comparison to the dispersion in the column.

Data treatment was done by fitting the solution of the axial dispersion model, Eq. (5), to the experimentally measured RTD using non-linear regression in time domain [27]. The values of absorbance directly read in the spectrophotometer were adopted as the tracer concentration (in arbitrary units), since the data treatment does not require absolute measurements of concentration. A sample of experimental and adjusted RTD curves is presented in Fig. 2.

5. Results and discussion

A set of 213 planned runs were carried out, in the range of pulsing amplitude 5, 10, 15, 20 and 25 mm; pulsing frequencies from 0 to 4.5 s^{-1}; plate spacing 25, 50 and 100 mm, and flow rate 3.8, 5.5, 7.5, 9.9 and 11.8 l/h.

5.1. Reproducibility

Table 1 presents the values obtained in replicated experiments, showing good reproducibility. Flow rate and pulsing frequencies presented S.D. not higher than 0.34 and 0.87% of the respective average values, the worse values are within 2.0 S.D. Pulsing amplitude was adjusted once at each run and its error was lower than 0.5 mm. Also good reproduction can be seen for the axial dispersion coefficients, the worse reproducibility for those obtained under no pulsation (zero frequency). The S.D. for D_{ea} were in the range from 6 to 11% of the average values, the worse values within 1.4–1.8 S.D. and the 95% confidence limits lie between 6 and 11% of the mean values.

5.2. Effect of frequency and amplitude of pulsation, flow rate and plate spacing in pulsed experiments

Figs. 3–5 show the effects of the pulsation frequency (f) and amplitude (A) for plate spacing $h = 25$, 50 and 100 mm,

Table 1
Reproducibility of axial dispersion coefficients in PSPC ($h = 50$ mm)

Run	Q (l/h)	f (s^{-1})	D_{ea} (cm^2/s)	$D_{ea,calc}$ (cm^2/s)[a]
B148	9.89	0.19	1.08	
B59	9.89	0.20	1.43	
B15	9.86	0.21	1.27	
B52	9.89	0.21	1.19	
B81	9.89	0.23	1.30	
Mean	9.88	0.21	1.25	0.54
S.D.	0.01	0.01	0.13	–
B12	11.82	2.28	2.72	
B50	11.85	2.28	2.65	
B66	11.85	2.28	2.53	
B72	11.78	2.28	2.71	
B95	11.82	2.31	3.00	
B104	11.88	2.33	2.72	
Mean	11.83	2.29	2.72	3.90
S.D.	0.03	0.02	0.15	–
B108	11.85	4.45	4.05	
B101	11.90	4.48	4.71	
B107	11.88	4.49	3.98	
B09	11.79	4.50	4.56	
B87	11.88	4.50	5.24	
B97	11.83	4.53	4.33	
B105	11.87	4.54	5.06	
Mean	11.83	4.50	4.56	7.19
S.D.	0.03	0.03	0.48	–

[a] OBS: $D_{ea,calc}$ was calculated by the correlation, Eqs. (7) and (9).

respectively, at flow rate $Q = 11.8$ l/h. For moderate and high values of amplitude (10–25 mm), the axial dispersion coefficient increases as the pulsation frequency increases. For lower values of amplitude ($A = 5$ mm), the axial dispersion coefficient is practically not affected by pulsation frequency. According to the isotropic turbulence theory by Kolmogoroff [28], the axial dispersion coefficient is related

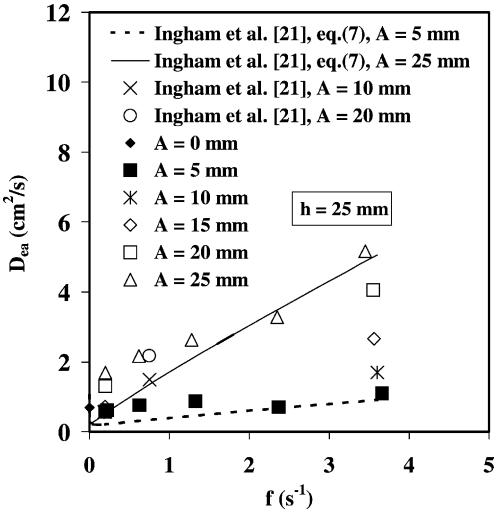

Fig. 3. Effect of pulsing frequency and amplitude on the axial dispersion coefficient ($Q = 11.8$ l/h, $u = 0.267$ cm/s, $h = 25$ mm).

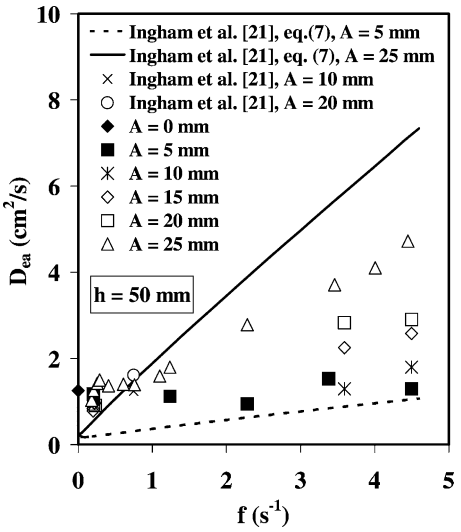

Fig. 4. Effect of pulsing frequency and amplitude on the axial dispersion coefficient ($Q = 11.8$ l/h, $u = 0.267$ cm/s, $h = 50$ mm).

to the Prandtl mixing length, l, and the power dissipation in a system due to mechanical agitation, P, by the following equation:

$$D_{ea} = l^{4/3} P^{1/3} \tag{10}$$

$$P \propto (Af)^3 \tag{11}$$

According to Eq. (10), D_{ea} would increase with P and l. However, the increase of P promotes turbulence and mixing of the flow and consequently l decreases. From Figs. 3–5 we can see that for $A = 5$ mm the decrease of l compensates the increase of f, so the D_{ea} values remains almost constant for the f range studied. For $A = 25$ mm there is a small decrease of l with the increase of f, so we can observe a net increase of D_{ea} with f. This influence of A may be due to the presence of the perforated plates. The increase of A favors

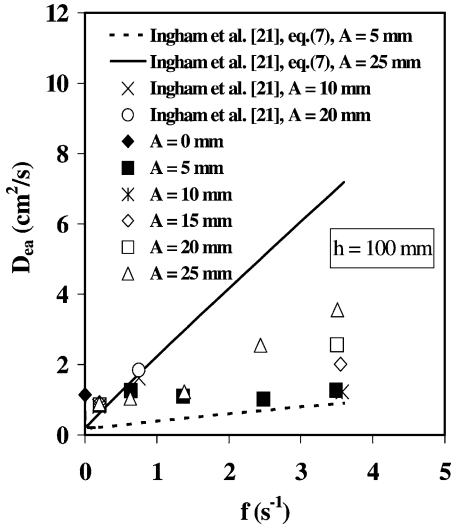

Fig. 5. Effect of pulsing frequency and amplitude on the axial dispersion coefficient ($Q = 11.8$ l/h, $u = 0.267$ cm/s, $h = 100$ mm).

the increase of mixing, so l decreases strongly already for small values of f. The greater the relation A/h the greater the D_{ea} values.

Axial dispersion coefficients are about 1.5 times higher for plate spacing $h = 25$ mm than for $h = 50$ mm, for amplitude $A = 25$ mm; for smaller values of amplitude the differences diminish and for amplitude $A = 5$ mm they are practically equal for all plate spacing studied. For plate spacing $h = 100$ mm, the axial dispersion coefficient are rather smaller than that for $h = 50$ mm. Similar behavior was observed for other flow rates (not shown).

We can observe in Fig. 4, for small values of pulsation frequency, there is a decrease of the axial dispersion, followed by a slight increase. This may be due to the decrease of the mixing length, as suggested by Ni and Pereira [29]. According to these authors, the introduction of pulsation increases the mechanical energy dissipation to the system, which breaks up eddies and reduces the mixing length, and thus the dispersion coefficients. From this point on, the increase of pulsation causes an increase in turbulence and axial dispersion.

For sake of comparison, two experimental data obtained by Ingham et al. [21] were also included in Figs. 3–5. These data were originally under zero flow conditions and were corrected to flow rate $Q = 11,8$ l/h using Eq. (9). There is a fair agreement to the experimental data obtained in the present work for plate spacing $h = 25$ and 50 mm. However for plate spacing $h = 100$ mm, the data obtained by Ingham et al. [21] are about two times higher than that obtained in the present work. Figs. 3–5 also show the predictions by the correlation of Ingham et al. [21], given by Eq. (7) and (9). The qualitative trend of increase of D_{ea} with both the pulsing frequency and amplitude predicted by the correlation is observed in Figs. 3–5 for plate spacing $h = 25$, 50 and 100 mm. The quantitative predictions of the axial dispersion coefficients are in good agreement to our results for plate spacing $h = 25$ mm for moderate to high values of pulsation frequency. For plate spacing $h = 50$ and 100 mm, the predicted values are higher than our results for amplitude $A = 25$ mm, and smaller for amplitude $A = 5$ mm. The difference increases with plate spacing. The correlation of Ingham et al. [21] is unable to predict the value of axial dispersion for non-pulsed flow ($f = 0\,s^{-1}$) because it exhibits a discontinuity at this point.

Fig. 6 shows the effects of the flow rate and plate spacing, for high pulsation intensity, at pulsation amplitude $A = 25$ mm and frequency $f = 3.5\,s^{-1}$. There is a clear (yet small) trend of experimental values of D_{ea} increasing linearly with flow rate. As pointed out by Ingham et al. [21], under many practical circumstances $u \ll 2Af$, so the effect of flow rate is not expected to be large. The highest experimental values of D_{ea} are that for $h = 25$ mm; no significant difference can be observed for $h = 50$ and 100 mm.

The calculated results by the correlation of Ingham et al. [21] and Miyauchi and Oya [16], also shown in Fig. 6, predict higher D_{ea} values than the experimental values and are

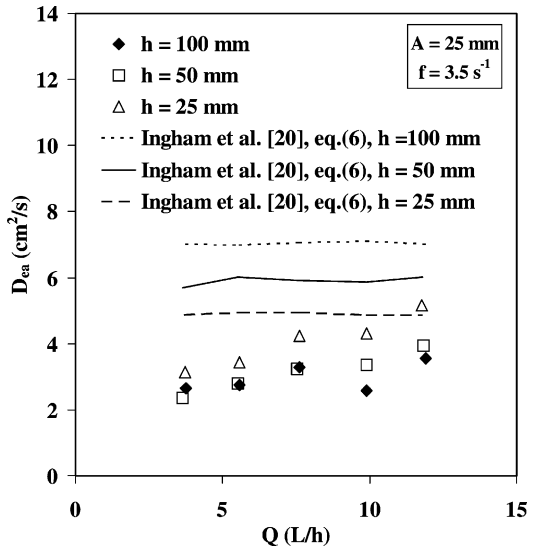

Fig. 6. Effect of flow rate Q on the axial dispersion coefficient ($A = 25$ mm, $f = 3.5\,s^{-1}$, u (cm/s) $= 2.256 \times 10^{-2}$ Q (l/h)).

almost insensitive to the flow rate. More significant is the fact that the correlation predicts an increase of D_{ea} with h, which is not observed from the experimental data.

According to Ni and Pereira [29], the flow rate also contributes to the increasing of D_{ea} through the increase of the mechanical energy dissipation, due to the presence of perforated plates, and, consequently, the mixing length increases. However, the mixing length is much less affected by the flow rate than by the pulsation intensity.

Fig. 7 shows the effect of the flow rate and plate spacing, for low pulsation intensity, at pulsation amplitude $A = 5$ mm and frequency $f = 0.2\,s^{-1}$. There is a small decrease in D_{ea} at low flow rates, and then an increase of D_{ea} with flow rate. The lowest experimental values are those for $h = 25$ mm, while it was expected to have the greatest D_{ea} for this plate spacing. The calculated D_{ea} values by the correlation of Ingham et al. [21] and Miyauchi and Oya [16], also shown in Fig. 7, predict lower values than the observed ones. The correlation predicts almost the same D_{ea} values for the three plate spacing values, because the sensitivity of the correlation diminishes for low pulsation intensity.

From Fig. 7, for $h = 50$ and 100 mm, it can be observed a decrease of D_{ea} for small values of flow rate, followed by a slightly increase. This may be due to the change of the flow patterns, as laminar to transition flow regime, with increasing flow rate. The mixing length decreases as the flow rate increases and eddies break up. From this point on, the increase of flow rate increases the turbulence and the axial dispersion.

From Figs. 6 and 7 we observe a trend inversion regarding the effect of plate spacing from high to low pulsation intensity, due to the change of flow patterns. From Fig. 6 the axial dispersion for $h = 25$ mm is smaller than that for $h = 50$ and 100 mm, which is caused by the smaller mixing length for $h = 25$ mm. The D_{ea} values increase with flow rate as a consequence of the mechanical energy dissipation due to the plates.

5.3. Effect of flow rate and plate spacing in no-pulsed experiments

Fig. 8 shows the results for zero frequency (no-pulsed experiments) obtained for two different flow velocity (u) and three different plate spacing (h) values. The axial dispersion coefficient increases with plate spacing from $h = 25$ to 50 mm for the two flow rates studied; the D_{ea} values diminish with plate spacing from $h = 50$ to 100 mm. The axial dispersion coefficient increases with u and exhibits a maximum for intermediate values of plate spacing.

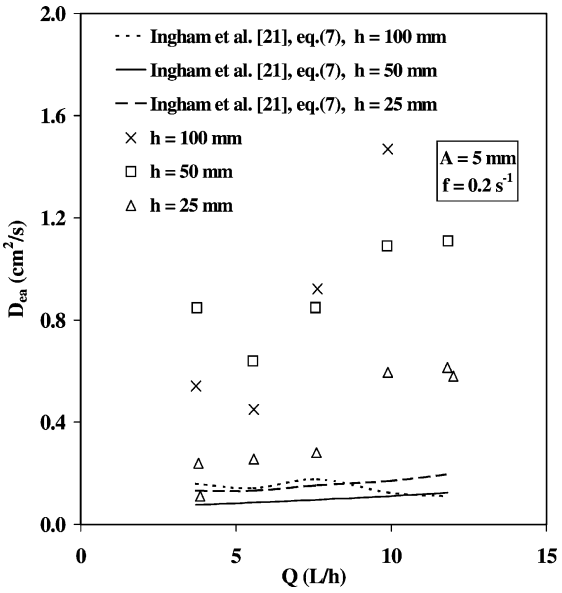

Fig. 7. Effect of flow rate Q on the axial dispersion coefficient ($A = 5$ mm, $f = 0.2\,s^{-1}$, u (cm/s) $= 2.256 \times 10^{-2}$ Q (l/h)).

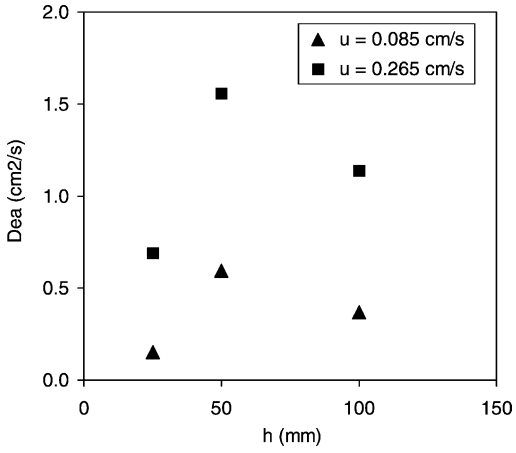

Fig. 8. Effect of the flow velocity (u) and plate spacing (h) on the axial dispersion coefficient, for non-pulsed flow (system without pulsation).

From Fig. 8 we observe a trend inversion for $h = 100$ mm which denotes flow pattern change inside the PSPC. Analyzing the results of Fig. 8 in terms of mixing length, we can say that the mixing length grows from $h = 25$ to 50 mm and decreases from $h = 50$ to 100 mm for the two velocities studied. The reasons for this behavior could be better understood through the CFD studies.

It is interesting to note that the plate spacing has opposite effects in systems with and without pulsing. For pulsed systems, higher dispersion coefficients were observed for the lowest plate spacing, while for no-pulsed systems an increase in plate spacing results in maximum value of axial dispersion coefficients.

5.4. Effect of viscosity in pulsed experiments

Fig. 9 shows the effect of viscosity for plate spacing $h =$ 25, 50 and 100 mm, obtained for pulsation amplitude $A =$ 25 mm, pulsation frequency $f = 3.5\,s^{-1}$ and at flow rate $Q = 11.8$ l/h. Experiments with different viscosity may be important to model the polymerization process occurring in this column when operating as a continuous reactor, since polymer emulsions have higher viscosity than that of water. At the concentration range used, the rheological behavior of the aqueous solutions of poly(vinyl alcohol) is similar to that of a Newtonian fluid. This kind of solution mimics reasonably well the viscosity and rheological behavior of polymer emulsions with low solid contents, which also present close to Newtonian characteristic.

For plate spacing $h = 25$ mm, the axial dispersion increases with viscosity. For plate spacing $h = 50$ mm, there is no clear trend of dependence of the viscosity. For plate spacing $h = 100$ mm, it seems that the axial dispersion first decreases and then increase with viscosity, passing through a minimum.

Fig. 9 also shows the predicted values given by the correlation of Ingham et al. [21], Eq. (7). The correlation overestimates the values of axial dispersion for plate spacing 50 and 100 mm, the higher the plate spacing the greater the difference between predicted and experimental values. The correlation reproduces well the results for plate spacing 25 mm and for viscosity values up to 4.0 cP. The correlation shows a slight tendency of increasing the axial dispersion with the viscosity, which agrees with our observations. The fall observed in the experimental values of axial dispersion in Fig. 5 for plate spacing $h = 50$ and 100 mm and viscosity 2.3 cP may be due to the decrease in the mixing length, as suggested by Ni and Pereira [29]. The increase of the viscosity increases the mechanical energy dissipation to the system, which breaks up eddies and reduces the mixing length, and thus the dispersion coefficients.

As the effect of viscosity on D_{ea} is small in the range studied (1–10 cP), values of D_{ea} obtained for water at 20 °C can be used for low solid-content polymer emulsions, that have similar viscosity at typical polymerization temperatures (50–65 °C).

5.5. Correlation through dimensionless groups

A first attempt on correlating the joint effects of variables on the axial dispersion coefficient is presented in Fig. 10. The plot of the dimensionless group $D_{ea}/(uh)$ versus the dimensionless group Af/u resulted in three fairly well-behaved trends for each plate spacing ($h = 25$, 50 and 100 mm). The group $D_{ea}/(uh)$ can be recognized as the inverse of a modified Peclet number for the column. This group increases as Af/u increases. All data could be represented, in a first approximation, by one curve for each value of plate spacing.

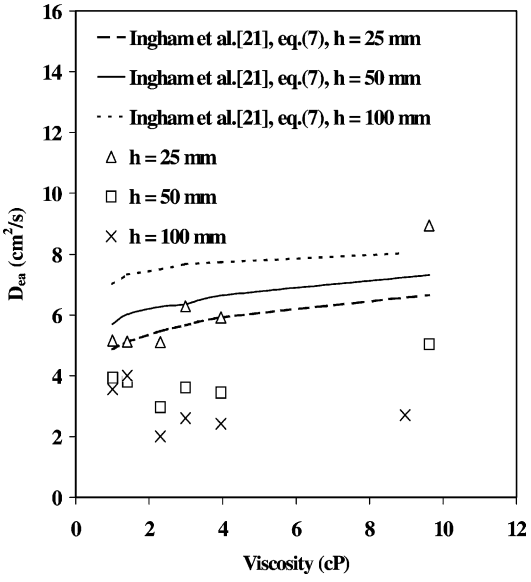

Fig. 9. Effect of the viscosity on the axial dispersion coefficient for pulsed flow ($A = 25$ mm, $f = 3.5\,s^{-1}$, $Q = 11.8$ l/h, $u = 0.267$ cm/s).

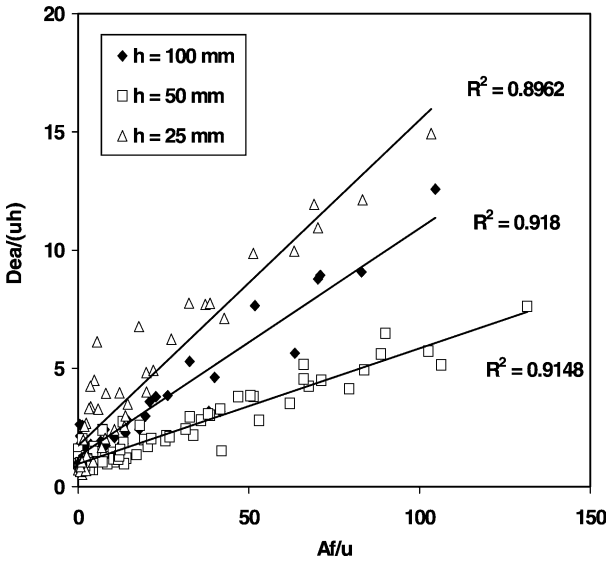

Fig. 10. Correlation of all experiments with water.

Linear regression curves for each plate spacing are plotted in Fig. 10. The effect of the other variables (A, f, and u) seems to be reasonably accounted for by these two dimensionless groups, although the inclusion of the same variable (u) in both dimensionless groups always favors the appearance of certain degree of correlation, as discussed by Rowe [30].

Since Af is the pulsing velocity and u is the convective velocity, the group Af/u is the relation between the pulsing and convective velocity. This dimensionless group can be recognized as the relation between the oscillatory Reynolds number and the net flow Reynolds number, as defined by Ni and Pereira [29]. For great values of Af/u the flow patterns in the column are governed by pulsation while bulk flow convection is more important for low values of Af/u. Although it would be expected such a flow regime change as a function of Af/u, Fig. 10 does not show any recognizable trend to confirm such behavior.

We can observe in Fig. 10 that the curve for plate spacing $h = 100$ mm lies between the curves for plate spacing 25 and 50 mm, revealing a complex and somehow intriguing behavior. This may be due to changes of the fluid dynamic behavior in the column as plate spacing changes. Further studies are required in order to offer a sound interpretation for this point.

5.6. Effect of sampling probe position

Some experiments were performed in order to access if sampling probe position would affect the results. Table 2 presents a sample of these results, for repeated runs with flow rate 11.8 l/h and pulsing frequency 0.2 s^{-1}. In one series, the sampling point used was at the end of the first section ($z = 870$ mm) and in the second series the sampling point used was that at the end of the third section ($z = 2616$ mm). Practically, the same values of the axial dispersion coefficient were obtained in these two situations. Similar results were also obtained for other operating conditions, always the coefficients obtained for different axial sampling positions agree within the confidence interval of the estimates.

Table 2
Axial dispersion coefficients for different axial position of sampling point

Sampling point at $z = 870$ mm		Sampling point at $z = 2616$ mm	
Run	D_{ea} (cm^2/s)	Run	D_{ea} (cm^2/s)
B04	0.99	B54	1.08
B05	1.06	B56	1.15
B53	1.06	B63	1.42
B57	1.3	B83	0.93
B82	0.93	B86	1.02
B84	0.97	B140	0.92
B85	1.09	–	–
B58	1.22	–	–
Mean	1.08	–	1.09
S.D.	0.13	–	0.19

$h = 50$ mm, $Q_m = 11.8$ l/h, $\sigma_Q = 0.03$ l/h, $f_m = 0.2\ s^{-1}$, $\sigma_f = 0.01\ s^{-1}$.

In all cases the sampling tube was placed at the column wall. The radial position of the sampling tube is expected to play a role only for non-pulsating flow experiments, for which the radial mixing seems much less intense (this was visually observed during the experiments). Therefore, the results here reported for non-pulsating experiments should be interpreted in a qualitative or comparative fashion. For all pulsated flow experiments, even for the lowest pulsing frequency (0.2 s^{-1}) and the lowest flow rate (3.8 l/h), good radial mixing was visually observed (quite good radial spreading of the injected tracer).

6. Concluding remarks

An experimental study of axial dispersion in pulsed sieve plate column is presented. Good reproducibility of the data obtained in the experiments was observed. Axial dispersion coefficients in oscillatory flow increase as the frequency and amplitude of pulsation are increased. In experiments without pulsation (zero frequency), the axial dispersion coefficient presented a maximum value for an intermediate value of plate spacing. The influence of plate spacing is rather complex and deserves further studies. Simple linear correlation between the dimensionless groups $D_{ea}/(uh)$ and Af/u were presented for each plate spacing studied. The influence of the viscosity on the axial dispersion coefficients was rather small in the range studied.

The available correlation in the literature for axial dispersion coefficient in single-phase flow in PSPC was tested and was not able to correctly predict all the trends experimentally observed. For instance, the effect of plate spacing seems to be rather complex and calls for further experimental studies. In addition, numerical simulations by computational fluid dynamics (CFD) would be helpful in providing more comprehensive understanding of the pulsed flow in perforated plates, offering better insight in understanding the flow and the mixing in such system, as done by Ni et al. [31] for oscillatory flow in baffled column.

The axial dispersion coefficients ranged from 0.11×10^{-4} to $9 \times 10^{-4}\ m^2/s$, or Pe from 70 to 2.5, showing that the axial dispersion in the PSPC can be varied in a wide range and can be adjusted to drive the flow behavior approaching a PFR or a CSTR. This makes feasible the use of the PSPC as a number of applications; in particular our group has successfully used the PSPC as a continuous emulsion polymerization reactor, Sayer et al. [32] with clear advantages over the CSTR.

Acknowledgements

The financial support from Fundação de Amparo à Pesquisa do Estado de São Paulo (FAPESP) and Conselho Nacional de Desenvolvimento Científico e Tecnológico (CNPq) is gratefully appreciated.

References

[1] R.K. Greene, R.A. Gonzales, G.W. Poehlein, ACS Symp. Ser. 24 (1976) 341–348.
[2] C. Kiparissides, J.F. MacGregor, A.E. Hamielec, Can. J. Chem. Eng. 58 (1980) 48–55.
[3] G.F.M. Hoedemakers, Ph.D. Thesis, Technical University Eindhoven, Eindhoven, 1990.
[4] D.A. Paquet, W.H. Ray, AIChE J. 40 (73) (1994) 73–87.
[5] H.R.C. Pratt, M.H.I. Baird, Axial dispersion, in: T.C. Lo, M.H.I. Baird, C. Hanson (Eds.), Handbook of Solvent Extraction, Wiley, New York, 1983, pp. 199–247.
[6] A. Qader, G.W. Stevens, H.R.C. Pratt, Ind. Eng. Chem. Res. 37 (1998) 2087–2092.
[7] J.C. Mecklenburgh, S. Hartland, The Theory of Backmixing, Wiley, Bristol, 1975.
[8] O. Levenspiel, K.B. Bischoff, Patterns of flow in chemical process vessels, in: T.B. Drew, J.W. Hoopes, T. Vermeulen (Eds.), Advances in Chemical Engineering, Academic Press, New York, 1963, pp. 95–198.
[9] A. Kreft, A. Zuber, Chem. Eng. Sci. 33 (1978) 1471–1480.
[10] G. Brunello, R. Giudici, M. Palma, in: Proceedings of the XIII Brazilian Congress of Chemical Engineering and XIX Interamerican Congress of Chemical Engineering, Aguas de São Pedro, São Paulo, Brasil, 24–27 September 2000.
[11] C.Y. Wen, L.T. Fan, Models for Flow Systems and Chemical Reactors, Marcel Dekker, New York, 1975.
[12] M.T. Gouvea, S.W. Park, R. Giudici, in: Proceedings of the XVIII Encontro sobre Escoamento em Meios Porosos, Nova Friburgo, RJ, Brazil, 23–25 October 1990.
[13] M.S.A. Palma, R. Giudici, in: Proceedings of the Spring National Meeting, Houston, TX, USA, 22–26 April 2001, AIChE.
[14] W.J.D. Van Dijk, in: T.C. Lo, M.H.I. Baird, C. Hanson (Eds.), Handbook of Solvent Extraction, Wiley, New York, 1983, pp. 355–372; US Patent 201,186 (1935).
[15] D.H. Logsdail, M.J. Slater, Pulsed perforated-plate columns, in: T.C. Lo, M.H.I. Baird, C. Hanson (Eds.), Handbook of Solvent Extraction, Wiley, New York, 1983, pp. 355–372.
[16] T. Miyauchi, H. Oya, AIChE J. 11 (3) (1965) 395–402.
[17] P. Novotny, J. Prochazka, J. Landau, Can. J. Chem. Eng. 48 (8) (1970) 405–410.
[18] M.H.I. Baird, Can. J. Chem. Eng. 52 (12) (1974) 750–757.
[19] K.V.K. Rao, S.A.K. Jeelani, G.R. Balasubramanian, Can. J. Chem. Eng. 56 (2) (1978) 120–123.
[20] J.C. Godfrey, et al., Chem. Eng. Res. Des. 66 (9) (1988) 445–457.
[21] J. Ingham, et al., Trans. IChemE. 73 (7A) (1995) 492–496.
[22] M.A. Nabli, P. Guiraud, C. Gourdon, Chem. Eng. Sci. 52 (14) (1997) 2353–2368.
[23] J. Meuldijk, et al., Chem. Eng. Sci. 47 (9–11) (1992) 2603–2608.
[24] M.S.A. Palma, M.Sc. Dissertation, University of São Paulo, 1991.
[25] M.J.J. Mayer, J. Meuldijk, D. Thoenes, Chem. Eng. Sci. 49 (24B) (1994) 4971–4980.
[26] M.J.J. Mayer, J. Meuldijk, D. Thoenes, Chem. Eng. Sci. 51 (13) (1996) 3441–3448.
[27] D.W. Marquardt, J. Soc. Ind. Math. 11 (2) (1963) 431–441.
[28] A.N. Kolmogoroff, Akad. Nauk. USSR 30 (1941) 301–310.
[29] X. Ni, N.E. Pereira, AIChE J. 46 (1) (2000) 37–45.
[30] P.M. Rowe, Trans. Inst. Chem. Eng. (Lond.) 41 (1963) CE70.
[31] X. Ni, H. Jian, A.W. Fitch, Chem. Eng. Sci. 57 (2002) 2849–2862.
[32] C. Sayer, M. Palma, R. Giudici, Ind. Eng. Chem. Res. 14 (2002) 1733–1744.